The Cryosphere Discuss., 9, 2783–2820, 2015
www.the-cryosphere-discuss.net/9/2783/2015/
doi:10.5194/tcd-9-2783-2015

The Cryosphere Discussions
Open Access

Monitoring ice break-up on the Mackenzie River using MODIS data

P. Muhammad, C. Duguay, and K.-K. Kang

Department of Geography and the Interdisciplinary Centre on Climate Change (IC^3),
University of Waterloo, Waterloo, ON, Canada

Received: 20 March 2015 – Accepted: 13 April 2015 – Published: 20 May 2015

Correspondence to: P. Muhammad (pmuhamma@uwaterloo.ca)
and C. Duguay (crduguay@uwaterloo.ca)

Published by Copernicus Publications on behalf of the European Geosciences Union.

Abstract

This study involves the analysis of Moderate Resolution Imaging Spectroradiometer (MODIS) Level 3 500 m snow products (MOD/MYD10A1), complemented with 250 m Level 1B data (MOD/MYD02QKM), to monitor ice cover during the break-up period on the Mackenzie River, Canada. Results from the analysis of data for 13 ice seasons (2001–2013) show that first day ice-off dates are observed between days of year (DOY) 115–125 and end DOY 145–155, resulting in average melt durations of about 30–40 days. Floating ice transported northbound could therefore generate multiple periods of ice-on and ice-off observations at the same geographic location. During the ice break-up period, ice melt was initiated by in situ (thermodynamic) melt over the drainage basin especially between 61–61.8° N (75–300 km). However, ice break-up process north of 61.8° N was more dynamically driven. Furthermore, years with earlier initiation of the ice break-up period correlated with above normal air temperatures and precipitation, whereas later ice break-up period was correlated with below normal precipitation and air temperatures. MODIS observations revealed that ice runs were largely influenced by channel morphology (islands and bars, confluences and channel constriction). It is concluded that the numerous MODIS daily overpasses possible with the Terra and Aqua polar orbiting satellites, provide a powerful means for monitoring ice break-up processes at multiple geographical locations simultaneously along the Mackenzie River.

1 Introduction

The Mackenzie River Basin (MRB) is the largest in Canada and is subject to one of the most important hydrologic events annually. River ice break-up on the Mackenzie River is a process by which upstream (lower latitude) ice is pushed downstream while intact ice resists movement downstream (higher latitude) (Beltaos and Prowse, 2009). Ice break-up is defined as a process with specific dates identifying key events in space and time between the onset of melt and the complete disappearance of ice in the river. This is the definition used in previously published literature and which will be applied in this paper. Break-up is often associated with flooding in north flowing systems and is thus an important hydrologic event with many environmental benefits (e.g. geochemical land deposition and lake and groundwater recharge) and detriments (e.g. infrastructure damage and lost economic activity) (Prowse, 2001; Kääb et al., 2013). Investigations of river regimes in high latitude countries including Canada, the United States, Russia and Sweden and Finland have a long history related to their ice monitoring (Lenormand et al., 2002). This is important as ice freeze-up and break-up records serve as climate proxies responding to changing air temperature patterns (Magnuson et al., 2000). The ice break-up process is nonetheless under-monitored. There is therefore a gap in knowledge when attempting to understand all associated hydrologic parameters due to their highly dynamic nature (Beltaos et al., 2011).

The shortage of ice observations on the Mackenzie River and other rivers and lakes in Canada is partly the result of budget cuts, which have led to the closing of many operational hydrometric stations (Lenormand et al., 2002). Specifically, ice freeze-up and break-up observations peaked during the 1960–1990s and declined dramatically thereafter following budget cuts from the federal government (Lenormand et al., 2002). In the last decade only, the observational network of discharge and ice measurements on the MRB has declined from 65 to 15 stations. Satellite remote sensing is a viable tool for filling this observational gap. For example, Pavelsky and Smith (2004) were able to monitor ice jam floods and break-up events discontinuously over a 10 year period (1992–1993, 1995–1998, and 2000–2003) on major high-latitude north-flowing rivers at 500 m and 1 km spatial resolutions (the Lena, Ob', Yenisey and Mackenzie rivers) using MODIS and Advanced Very High Resolution Radiometer (AVHRR) imagery. Similarly, Chaouch et al. (2012) showed the potential of MODIS (0.25 and 1 km spatial resolutions) for monitoring ice cover on the Susquehanna River (40–42° N), USA, from 2002–2010. Kääb and Prowse (2011) and Kääb et al. (2013) have also shown the effectiveness of remote sensing data acquired at 15, 2.5 and 1 m spatial resolutions using Advanced Spaceborne Thermal Emission and Reflection Radiometer (ASTER), Panchromatic Remote-sensing Instrument for Stereo Mapping (PRISM) and IKONOS, respectively, for estimating river ice velocities. However, these previous studies have been limited to spaceborne stereographic datasets capturing a few ideal (cloud-free) images a year and including revisit times ranging from 2–16 days, making detailed temporal studies difficult. Despite these recent advances, studies have yet to be conducted monitoring ice freeze-up and break-up processes by satellite remote sensing over longer periods (i.e. continuously over several years).

The aim of the present study was therefore to develop an approach to estimate key ice break-up dates (or events) on the Mackenzie River (MR) over more than a decade using Moderate Resolution Imaging Spectroradiometer (MODIS) data. The paper first provides a description of the procedure developed to monitor ice break-up on the MR. This is followed by a quantification of ice-off dates (spatially and temporally) provided by MODIS data. Next, average ice-off dates are compared for a 13 year period (2001–2013). Lastly, displacement of ice runs calculated with MODIS is used to estimate average ice velocity along sections of the MR.

2 Methodology

2.1 Study area

The geographical area of this study focuses on the Mackenzie River extending from the western end of Great Slave Lake (61.36° N, 118.4° W) to the Mackenzie Delta (67.62° W, 134.15° W) (Fig. 1). The study area encompasses the main channel and confluences of the river, including any smaller rivers that feed the Mackenzie. Currently, only five hydrometric stations measure water level and ice on the main channel (1100 km long) of the Mackenzie River north of Great Slave Lake. The MRB forms the second largest basin in North America extending beyond the Northwest Territories at 1.8×10^6 km^2 (Government of Canada, 2007b). Approximately 75 % of the MRB lies in

TCD
9, 2783–2820, 2015

the zones of continuous and discontinuous permafrost with many smaller sub-basins adding to flow at different time periods during the break-up season (Abdul Aziz and Burn, 2006). The MRB experiences monthly climatological (1990–2010) averages of −20 to −23 °C air temperature between the months of December to February, respectively (Brown and Derksen, 2013). Air temperature increases to an average of −5 °C in April with the initiation of ice break-up near 61° N.

Air temperature plays an important role on the timing of spring freshet (Beltaos and Prowse, 2009; Goulding et al., 2009b; Prowse and Beltaos, 2002) in the MRB. It has therefore been associated with increased flow and the initiation of ice break-up in the basin as a result of snowmelt onset (Abdul Aziz and Burn, 2006). In thermal (overmature) ice break-up, there is an absence of flow from the drainage basin earlier in the melt season, and the ice remains in place or is entrained in flow until incoming solar radiation disintegrates the river ice increasing water temperatures (Beltaos, 1997). This slow melting process causes a gentle rise in discharge on a hydrograph, with flooding found to be less frequent during that period (Goulding et al., 2009a). In dynamic (premature) ice break-up, the accumulation of snow on the drainage basin is higher and the stream pulse (or spring freshet) from snowmelt is characterized by a high slope on the rising limb of the hydrograph (Goulding et al., 2009b; Woo and Thorne, 2003a). In the presence of thick ice downstream, flow can be impeded causing a rise in backwater level and flooding upstream. However, when ice resistance is weak downstream, stress applied on the ice cover can rise with increasing water levels fracturing and dislodging ice from shorelines continuing downstream, eventually disintegrating downstream (Hicks, 2009). This process can continue until certain geometric constraints such as channel bends, narrow sections and islands can stop the ice run causing ice jams (Hicks, 2009). Here, the wide-channel jam is the most common of dynamic events which develops from the flow shear stress and the ice jams' own weight, which is formed by the collapse and shoving of ice floe accumulation and is resisted by the internal strength of the accumulation of ice flows (Beltaos, 2008). As the jam builds with ice rubble, the upstream runoff forces can increase above the downstream

TCD
9, 2783–2820, 2015

resistance releasing the jam and creating a wave downstream that raises water levels and amplifies flow velocities (Beltaos et al., 2012). Observations have shown an initial increase and final decrease in water levels as wave celerity and amplitude attenuates downstream (Beltaos and Carter, 2009). In general, thermal decay and ice break-up process continue downstream after the ice jam release (Hicks, 2009). MODIS imagery has also shown the timing of spring flood and location of open water tributaries to have the most impact on ice break-up processes (Pavelsky and Smith, 2004).

2.2 MODIS data

MODIS images, for the period from one week before to one week after the ice break-up period had ended over the MRB from 2001–2013, were downloaded from the National Aeronautic and Space Administration's (NASA) Earth observing System Data and Information System (EOSDIS) (http://reverb.echo.nasa.gov/reverb/) for processing. This study used 500 m (primary data) and 250 m (secondary data) spatial resolution MODIS data acquired from both the Aqua and Terra satellite platforms. More specifically, MODIS L1B (MYD02QKM/MOD02QKM) and MODIS Snow Product (L3) (MYD10A1/MOD10A1) datasets were retrieved for analysis. In this paper, the MODIS will generally be referred to as L3 and L1B. L3 and L1B images were processed using the MODIS reprojection tool swath and MODIS conversion toolkit respectively, using UTM projection and nearest neighbor resampling. RGB true-color composites and near-infrared band – MODIS Band 1 (250 m, 620–670 nm), Band 4 (500 m, 545–565 nm) and Band 3 (500 m, 459–479 nm) as well as Band 2 (250 m, 841–876 nm) from MODIS L1B were selected. In each of the L3 and L1B available image sets, daily swaths were mosaicked independently and automatically processed.

If cross-sections of a river were observed to be clear of ice from bank to bank using (Terra/Aqua) L3 Snow Product, then one observation would be made for the particular geographic location and time. However, cloud cover presence was one of the few incidences where image processing was limited. This has also been previously reported (Riggs et al., 2000) where cloud cover in the Arctic limited data acquisition

TCD
9, 2783–2820, 2015

from the study site. This, in combination with coarse-resolution cloud cover masks resulted in 5–10 % of the images being omitted from analysis. Problems in snow detection arise when spectral characteristics important in the use of the normalized difference snow index (NDSI) make it difficult to discriminate between snow and specific cloud types (Hall et al., 2006). NDSI is insensitive to most clouds except when ice-containing clouds are present, exhibiting a similar spectral signature to snow. Hence, some MOD35/MYD35_L2 cloud mask images presented conservative over-masking of snow-cover on cloudy and foggy days (Hall et al., 2006).

To improve temporal coverage, ice-off observations were also carried out at varying overpass times (Chaouch et al., 2012) using MODIS L1B radiance products from both Aqua and Terra satellites, which do not include the MOD35/MYD35 cloud mask. If cloud cover was present in both L3 Terra and Aqua imagery, L1B images were used to make ice-off observations. Image sets from DOY 100 to 160 were analyzed to observe patterns over the entire ice break-up period ranging from 61 to 68° N. Ice-off observations were recorded at latitudes where ice was present but subsequently absent from images the next Julian day. North flowing ice could generate multiple ice-on and ice-off dates at the same geographic location. Ice-off and ice-on dates are dynamic ice run events during the ice break-up period. Multiple ice-off dates observed by satellite imagery were referenced and compared to specific hydrometric stations from the Water Survey of Canada (WSC) along the Mackenzie River (Table 1).

Furthermore, river sections where land and river features were mixed within pixels of the 500 m MODIS products were excluded. To minimize the amount of excluded pixels due to cloud cover and pixel mixing, MOD L1B images at a higher spatial resolution (250 m) were also used.

A region of interest (ROI) was delineated over the Mackenzie River where ice break-up was observed. MODIS L3 and L1B are provided as scientific data set (SDS) values and digital number (DN) values, respectively (Table 2). The MODIS L3 SDS values are described in the "MODIS Snow Product User Guide Collection 5" (Hall et al., 2006).

Matching SDS values on cloud free days were used to derive MODIS L1B DN threshold values.

2.3 Ice velocity

In addition to determining instances of ice break-up events with respect to location and time, this study also explored the use of MODIS as a tool for estimating velocity of ice flows. Ice velocity was observed and recorded on stretches of ice debris (> 15 km) where ice and water demarcation was distinguishable. At the demarcations, SDS values changed from 37 to 100 (open water to ice) at the leading edge and 100 to 37 (ice to open water) at the following edge of the north flowing river ice. Velocity was estimated by tracking the displacement of ice over time across multiple MODIS L3 and L1B swaths. Displacement estimates over time were made twice daily from Aqua and Terra satellites, although there is no way of telling that ice was moving within each MODIS image capture. Average velocities were recorded until ice debris could no longer be distinguished as a result of melt processes or when ice and open water were otherwise unobservable due to the presence of cloud cover. Ice velocities recorded also represent the lower limit of the ice flows, as the ice may not be moving at all times between image acquisitions. Therefore, the average velocities present time periods when the ice could be at rest and, therefore, the velocity measurements represent underestimation of the actual ice velocities. Ice debris movement was also referenced to WSC station provided that an operational station was on the route of the ice run.

3 Results

3.1 Thermal and dynamic ice break-up

The use of L3 imagery from a single MODIS sensor (Aqua or Terra) limited the potential to acquire continuously ice break-up observations as a result of cloud cover conditions. In some years, this represented up to 40 % of unusable imagery required to measure

TCD
9, 2783–2820, 2015

river ice-off dates. However, by using L3 product from both Aqua and Terra satellites across varying orbital tracks in combination with the L1B product greatly increased the number of observable events during ice break-up period, up to more than 90 % of available images. MODIS acquisitions from both the Aqua and Terra satellites doubled the number of images available during clear-sky conditions. In addition, the availability of MODIS L1B data from Aqua and Terra further increased the number of available images for analysis (i.e. cases where ice could be seen under thin clouds).

Over the 13 years of analysis, the ice break-up period ranged from as early as DOY 115 and lasted as late as DOY 155. Most ice break-up over the 13 year period (2001–2013) began between DOY 115–125 and ended between DOY 145–155. River morphology acted as an important spatial control determining the type of ice break-up process and ice run. Ice break-up processes between years showed different overall patterns with respect to location, thus temporally the beginning, end and duration of ice break-up varied. For example, the initiation of ice break-up in 2002 (Fort Simpson-330 km) began 10 days later than the average date when ice would completely clear the river section. Compared to 2007, the initiation of ice break-up began 13 days earlier than the average ice-off date at 270 km (61.57° N). As seen in Fig. 2, ice break-up initiates earliest at the headwaters (headwaters at 120 km, 61.43° N to 345 km, 61.92° N) between the Martin River and Mill Lake, and proceeds northward towards the Mackenzie Delta (see Fig. 3).

The initiation of the ice break-up period on the Mackenzie River was generally observed at the Liard River (325 km). The beginning and end of ice-off observations were observed to take place sooner near the Liard River than upstream and downstream of this location (Fig. 4). The confluence where the Mackenzie River and Liard River meet (61.82° N, 325 km) serves as a point where ice break-up proceeds dynamically northbound and thermodynamically southbound. South of 325 km, ice break-up was observed to be driven by a thermodynamic ice break-up regime (Fig. 6). So, ice break-up advanced opposite to the direction of river flow, southbound towards Great Slave Lake. Interestingly, higher frequencies of observations were observed south of 325 km where thermodynamic ice break-up regime was prevalent. This ice break-up "reverse" to the river flow was observed to continue until it approached Mill Lake, where the ice break-up was simultaneously progressing in the direction of flow. The converging course continued until no ice remained south of Martin River (Fig. 6).

As ice break-up proceeded northbound from the MR-Liard confluence, dynamic ice break-up flushed the ice downstream in a shorter period of time than the thermodynamic ice break-up south of the confluence (Figs. 2 and 3). Generally, however, distances above 560 km (63.22° N) (Wrigley, NWT) on the Mackenzie River experienced later ice break-up dates over the 13 years studied (Fig. 4).

Between 350–682 km (61.96–64° N) and north of the Mackenzie River and Liard River confluence, the average ice-off date for the study period was observed at DOY 130. The river width between 350–682 km was found to be smaller than reaches upstream (feeding ice into the main river channel) and downstream (letting ice exit the channel) as seen in Fig. 5. Consequently, the movement of ice into this river reach was limited causing ice entering the channel to jam while ice exiting the channel present from the winter period cleared sooner. There is also the possibility that the release of ice javes (river waves generated from ice jam) at the entrance of the channel could give rise to the rapid clearance of downstream ice over 1–2 day period over this 230 km stretch of the Mackenzie River (Beltaos et al., 2011).

Downstream of 682 km (64° N), river sections showed diagonal ice-off observations as seen in Figs. 2 and 3. These patterns are most visible in 2001, 2007–2009 and 2011–2012 observed between 860–1460 km (65–67.62° N). Observations of these diagonal events were the result of a second channel constriction at The Ramparts (1078 km, 66.19° N) as seen in Fig. 5, preventing northerly ice run. Here, the river channel decreased from 4 km to less than 0.5 km in width. It is hypothesized that ice runs downstream of The Ramparts (as a result of an ice jam) gave rise to similar ice-off dates (estimated at the southern ice-water boundaries of these flows) to ice runs towards The Ramparts. It is estimated that ice jams due to sudden decreases in river width as seen in 2001, 2007–2009 and 2011–2012 gave rise to earlier ice-off dates for river sections north of the jam resulting in impeded ice run which would normally maintain ice-on condition. This phenomenon resulted in a sequence of ice-off observations that occur simultaneously at two different latitudes, north and south of the ice jam. This further outlines the important morphological controls on the Mackenzie River over ice runs.

Based on MODIS imagery, ice break-up began on average between DOY 115 and 125 and ended between DOY 145 and 155 (Fig. 4). The standard deviation of estimated ice-off dates decreased with increasing latitude. MODIS derived dates showed highest deviations across river sections where thermodynamic ice break-up was prevalent. These patterns are similar to those seen from average break-up and standard deviations observed from the WSC. The 13 year average reveals similar ice conditions in the low, mid and high latitude of the Mackenzie River from MODIS and WSC data. There was an observed difference of 5 days between ice break-up observed from MODIS imagery and WSC. Also, the respective standard deviations overlap across the similar periods. Ice break-up in general continued in a north to south direction over the ice break-up periods. Near Forth Simpson (330 km, 61.85° N), it is worth mentioning that ice break-up was observed earlier than at more southern latitudes as illustrated by MODIS observations. This pattern is likewise visible from the WSC data.

Inter-annual variability of estimated average ice-off dates can be contrasted against ERA-interim 2 m height air temperature and precipitation data available until 2011 only (Brown and Derksen, 2013). As seen in Fig. 7, 2001, 2003, 2005–2007 and 2010 experienced earlier than normal (i.e. DOY 128) ice break-up dates. Furthermore in 2002, 2004, 2008–2009 and 2011 the average ice break-up date was estimated to be later than normal (DOY 128). Generally, years that experienced earlier than normal average ice break-up dates coincided with warmer (positive anomaly) than normal (−14.4 °C) air temperature or above normal (314 mm) precipitation (positive anomaly) or both from the preceding winter months (January to March). Conversely, later than normal ice break-up periods corresponded to below normal air temperature (negative anomaly) or precipitation (negative anomaly) or both.

TCD
9, 2783–2820, 2015

It is important to note that until 2010, five ground-based ice observation stations were operational on the MR. Following 2010, the hydrometric station on Mackenzie River at Fort Providence (61.27° N, 117.54° W, 75.8 km) was shutdown (Government of Canada, 2010b). Therefore, the WSC data was limited to 4 stations (Mackenzie River at Forth Simpson, Strong Point, Normans Wells, and Arctic Red River) in 2011 and 2012.

3.2 River ice velocity

Figures 8 and 9 illustrate ice movement from which ice velocities could be estimated over periods of 3–4 days following secondary channel constriction at 66° N. Here, ice runs that contained over 15 km of entrained ice were chosen to estimate average ice velocities. Only periods with at least three images with partial or no cloud cover were selected for velocity estimates.

In 2008, the open-water/ice boundary (leading edge) was recorded beginning on DOY 143 (Fig. 8). The open-water/ice (northern edge of ice) and ice/open-water (following edge) boundaries were both visible from DOY 144. Finally, the ice/open-water boundary was last observed on DOY 145. The average ice run velocity between 1063–1210 km (66–66.95° N) over the three days was estimated to be at least 1.21 $m s^{-1}$. Likewise, in 2010 (Fig. 9), open-water/ice (leading end) and ice/open-water (following end) was observed between DOY 138–141. The leading edge of the ice was first observed on DOY 138 and on DOY 139 when both the leading and following edges are visible. Finally, by DOY 141 the ice run has exited into the Mackenzie Delta. Across the 4 day period average ice run velocity was estimated to be at least 1.84 $m s^{-1}$.

TCD
9, 2783–2820, 2015

4 Discussion

4.1 Ice break-up and snowmelt relation

In order to assess the relative timing of ice disappearance in relation to its surrounding sub-basin, the timing of river ice disappearance was qualitatively compared to the timing of near complete snow disappearance from the surrounding area. MODIS L3 imagery of different years was selected which clearly revealed ice–snow relation with respect to location, where cloud cover was a minimal issue.

Locations where thermodynamic ice disappearance was hypothesized (south of 61.8° N, 325 km) corresponded with patterns where ice disappeared much later than snow on land (Fig. 6). For example, DOY 121/2006 (Fig. 10) was observed to be the beginning of the snowmelt period at 290–487 km (61.75–62.5° N) and this process ended when the snow had almost completely disappeared by DOY 125. However, DOY 125 corresponded to the initiation of ice break-up. This was not limited to 2006 so that snow generally disappeared sooner from surrounding sub-basins, followed by the initiation of ice-break-up.

At reaches north of the MR-Liard River confluence, ice break-up and snowmelt was observed to initiate in sync to one another. As seen in Fig. 11, on DOY 136–137/2011, ice disappearance on the southern cross-section of the figure is marked by the near simultaneous disappearance of snow. In fact by DOY 140/2011 both ice and snow had completely disappeared analogous to each other. On sections of the Mackenzie River before it enters the Mackenzie Delta, estimated ice break-up and snow disappearance was again observed to occur almost simultaneous to one another (Fig. 12). Over a 6 day period (DOY137–142/2007) the ice break-up process continued until ice completely disappeared from the channel (MR). This process ensued sooner relative to complete snowmelt over the surrounding sub-basins. By DOY 142/2007 nearly one-third of the river was completely cleared of ice while most of the snow was still present over the MRB.

Principally, it was concluded that on the upper Mackenzie Basin snow cleared sooner than the initiation of ice break-up. In the mid-Mackenzie Basin (375–860 km, 62 to 65° N), river ice cleared in-situ to snow clearance from the surrounding basin. In fact, ice cleared sooner in the mid basin than the upper Mackenzie Basin. Finally, in the lower Mackenzie Basin, river ice cleared sooner than the snow from the surrounding basin. This could be telling of a river continuum of the build-up of mechanical strength used to clear river ice within the Mackenzie River towards higher latitudes. The Liard River tributary accounts for one third of the total Mackenzie discharge (Woo and Thorne, 2003a), and so a rise in discharge in May initiates earlier ice break-up downstream as a result of increased stress induced on ice by a rise in river stage. Mechanical stress used to shove ice is continually magnified by the addition of small and large tributaries downstream of the Mackenzie River (Great Slave River, Arctic Red River).

Similar processes have also been observed on the Susquehanna River, USA, where an observed increase in discharge downstream foster earlier ice break-up while sections of upper river remain ice covered (Chaouch et al., 2012). The severity of ice break-up stage is therefore largely controlled by upstream discharge (Goulding et al., 2009b). Pavelsky and Smith (2004) also observed irregularities in ice break-up timing between years, particularly at 325 km (MR-Liard confluence) on the MR. Here, ice break-up began earlier at distances north of 325 km (61.8° N) than river sections south. Postponed ice break-up in the upper Mackenzie can result from the lack of discharge required to initiate ice break-up and so the ice is thermodynamically disintegrated.

4.2 Spatial and temporal ice break-up patterns

Over the 13 year period, the average estimated ice break-up dates were found to range between DOY 115–155 between distances 60 and 1460 km. These estimates from MODIS are in agreement with break-up dates reported by the WSC ground-based network. Previous studies on the MR, between the late 1930's to 2002, have found the initiation of ice break-up to range DOY 123–140 between 0 and 1217 km (de Rham et al., 2008a). Furthermore, it was reported by de Rham (2008b) that the duration of average ice break-up ranged from 8–10 days over the entire basin. With respect to the findings reported in Fig. 4, the observed ice-break-up patterns agree, such that the average observed break-up dates over the 13 year period ranged from DOY 128 ± 8 days at 61.5° N (260 km) to 145 ± 4 days at 68° N (1460 km). Others have reported, using MODIS and AVHRR imagery acquired between 1992 and 2002, that ice break-up ranged between DOY 120 and 155 (Pavelsky and Smith, 2004). The earliest reports of mean ice break-up dates ranged from 15 May (DOY 135) to 25 May (145) (1946–1955 averages), from Fort Providence to Arctic Red River, respectively (MacKay, 1966). Furthermore, others have reported a range of ice break-up dates from 22 May (DOY 142) to 31 May (DOY 151) (1927–1974, Fig. 2) from Fort Providence to Fort Good Hope, NWT, respectively (Allen, 1977).

In the headwaters of the Mackenzie River, ice break-up initiates the earliest between Mill Lake (120 km, 61.43° N) and Martin River (345 km, 61.92° N). As seen in Figs. 2–4, ice break-up between 120–300 km initiated earlier as compared to other sites on the Mackenzie River, but ice cleared later than other for other river sections downstream. Here ice in the channel remains stagnant for extended periods of time as ice usually freezes to bed and is most susceptible to thermodynamic melt (MacKay and Mackay, 1973).

Furthermore, at the Liard River confluence (325 km, 61.84° N) it was found that the seasonal initiation of ice break-up began and cleared earliest at this central location where the Liard River converges into the MR. Others (Pavelsky and Smith, 2004) have noted that at the MR-Liard River confluence flooding is common between years, especially near channel junction. Ice break-up at the Liard River confluence occurs rapidly, as the flow contribution is of greater magnitude than the Mackenzie River (MacKay and Mackay, 1973). This causes a lifting of the river stage, exerting pressure on the ice cover resulting in ice jam downstream most attributed to presence of channel bending (Camsell Bend, 456 km) and channel constriction.

Channel morphology is, therefore, a more important control on ice break-up patterns than previously believed. Both Pavelsky and Smith (2004) and de Rham et al. (2008a) alluded to the fact that channel morphology may exert influences on the patterns of ice break-up. In this study, it is determined that channel constriction at 350–682 km (61.96–64° N) and 1078 km (The Ramparts) is responsible for the delay of ice break-up timings upstream while promoting earlier ice break-up downstream. Upstream of the Liard River junction, river flow is stable. However, excessive discharge supplied by the Liard River causes earlier ice break-up and ice jamming downstream when the channel constricts between 350–682 km (MacKay and Mackay, 1973). Furthermore, excess supply of ice cover from the Great Bear River (821 km) into the Mackenzie River, causes the development of ice jamming at The Ramparts when the channel width decreases from over 3.5 km to less than 0.6 km (as seen in Fig. 5) (MacKay and Mackay, 1973).

Ice jamming from channel width decreases gave rise to similar sequences of ice-off observations, which occurred in tandem at two different latitudes, north and south of the ice jam (as seen at The Rampart). Ice jams are therefore favorable where morphological features impede downstream ice passage (Beltaos, 1997). These ice jams are caused by channel constriction resulting from mid-channel islands and narrow reaches (Terroux et al., 1981). Channel braiding, constriction and changes in slope have also been reported to be important factors influencing ice break-up and flow regimes (de Rham et al., 2008a). In the context of our study, it was found that channel constrictions and bends represented locations where ice runs were impeded. Hicks (2009) also reported that running ice may be stalled when geometric constraints such as tight bends, narrow sections and islands are present in rivers. In fact, it has been shown that ice debris flow drop to a velocity of zero in the presence of flow depths near channels islands and bars (Kääb et al., 2013). Lastly, Kääb and Prowse (2011), using ALOS PRISM stereo imagery on the Mackenzie River determined that ice velocities decrease to zero in the presence of bars.

The estimated ice run events illustrated in Figs. 7 and 8 may have been caused by ice jam releases (javes) initiated at The Rampart (1078 km, 66.19° N). Such processes may also be the reason why ice was estimated to be cleared at higher latitudes before the end of the snowmelt period. Accumulated stress with the rise of water levels behind the jam can result in sufficient kinetic energy to clear river ice downstream before the complete snowmelt overlying the surrounding sub-basins.

4.3 Ice velocities

Ice run velocities are believed to be the highest where the ice is minimally effected by channel morphology; unconnected from incoming tributaries; and channel splitting which causes the formation of islands (Kääb et al., 2013). Amongst the variety of ice runs observed over the 13 years, ice velocities could be quantified in 2008 and 2010. Over 3–4 day periods, average ice velocities were estimated to be 1.21 $m\,s^{-1}$ (2008) and 1.84 $m\,s^{-1}$ (2010). More importantly, it is believed that the evolution of such velocities is the product of javes. Our measurements of ice run velocity in 2008 coincidently synchronize with other independent satellite- and ground-based ice measurements. Extensive measurements of ice runs in 2008 around MR-Arctic Red River junction is believed to be generated by waves released from released ice-jams (Beltaos, 2013). This aligns with ice jams, which may form at The Rampart (1078 km, 66.19° N) as a result of channel constriction. The evolution of ice runs north of The Rampart (flowing past the Arctic Red River) observed over DOY 143–146/2008 (22–25 May/1.21 $m\,s^{-1}$) matches similar ground measurements (1.7 $m\,s^{-1}$) made by Beltaos et al. (2012). Across the same cross-section of the MR, Kääb and Prowse (with imagery acquired 1–2 days earlier in 2008) estimated a preceding ice run ranging from 0–3.2 $m\,s^{-1}$. The highest flow velocities were outlined where ice debris flow was most concentrated on the outside turn of the river bend. Finally, in another independent study, Beltaos and Kääb (2014) found ice debris velocities to range between 1–2 $m\,s^{-1}$ using ALOS PRISM imagery in 2010. Again these high-resolution (2.5 m) image measurements compare quite well with our estimates from relatively coarse spatial resolution (250–500 m) MODIS imagery. Additionally, early investigations have reported that ice can clear at velocities of 0.27 and 0.44 $m\,s^{-1}$ at Fort Simpson and Fort Good Hope, respectively during the ice break-up season (Terroux et al., 1981).

MODIS is shown to be a viable tool to measure river ice velocities. However, this study found that certain preconditions are required to use MODIS to its fullest extent. With respect to the MR, ice velocities were only quantifiable above The Rampart. The presence of morphological controls and therefore river width shortening leading to impeded ice run prevented quantifying velocities, as leading river–ice demarcations were difficult to locate. However, it was possible to estimate the overall velocity by observing ice–open water boundaries. Lastly, it was determined that in order to measure ice run velocities without major disturbance with impeded flows with respect to river morphology, estimates with MODIS should be made north of The Rampart. North of The Rampart, river widths were generally observed to be largest with respect to other parts of the MR.

5 Conclusions

The aim of this study was to develop an approach to estimate ice break-up dates on the Mackenzie River over more than a decade using MODIS snow and radiance products. It was found that the initiation of ice break-up started on average between DOY 115–125 and ended DOY 145–155 over the 13 years analyzed. Thermal ice break-up was an important process driving ice break-up south of the Liard River. Conversely, north of the Liard, ice break-up was dynamically driven. The addition to discharge from the MR-Liard River confluence outlined a location where initial ice break-up began. Furthermore, morphological controls such as channel bars, river meandering and channel constriction were found to be important factors controlling ice runs and ice break-up.

MODIS is currently the most promising tool for frequent monitoring of river ice processes as ground-based stations along the Mackenzie River are continuously being closed. Operating aboard two satellites (Aqua and Terra), the MODIS sensor allows for multiple daily acquisitions simultaneously along extensive stretches of the MR. Furthermore, MODIS is proving to be a viable sensor for the monitoring of river ice as shown in this and other recent investigations (e.g. Chaouch et al., 2012). In this study,

Discussion Paper | Discussion Paper | Discussion Paper | Discussion Paper |

TCD

9, 2783–2820, 2015

Monitoring ice break-up on the Mackenzie River using MODIS data

P. Muhammad et al.

monitoring of ice break-up on the Mackenzie River with MODIS proved to be a robust approach when compared to WSC ground-based observations. MODIS observations also allowed for the analysis of basin level processes influencing ice break-up, including river morphology and snowmelt.

Finally, future research should focus on investigating river ice processes using a combination of ground-based and satellite-based sensors; particularly for examining relations between river morphology, ice strength and discharge. Data from these complementary technologies would be valuable in the context of an early warning system for municipalities where river ice break-up is an important spring event causing significant flood damage. As an example, the 2014 Canadian spring thaw witnessed a variety of river ice related infrastructure damages, including the dislodgement of a bridge on the Canaan River, New Brunswick, Canada ("Covered bridge floats away," n.d.). Furthermore, a multi-sensor approach using both optical and synthetic aperture radar (SAR) data would be advantageous in order to monitor ice river processes and floods in near real-time. Satellite data from recent and upcoming SAR (Sentinel-1 and RADARSAT Constellation) and optical (Sentinel-2 and Sentinel-3) satellite missions will make such monitoring possible in the near future.

Acknowledgements. This research was supported by a NSERC Discovery Grant to C. Duguay.

References

Abdul Aziz, O. I. and Burn, D. H.: Trends and variability in the hydrological regime of the Mackenzie River Basin, J. Hydrol., 319, 282–294, doi:10.1016/j.jhydrol.2005.06.039, 2006.

Allen, W. T. R.: Freeze-up, Break-up and Ice Thickness in Canada: Embâcle, Débâcle Et Épaisseur de la Glace Au Canada, Environnement Atmosphérique, Downsview, Ontario, USA, 1977.

Beltaos, S.: Guidelines for Extraction of Ice-Breakup Data from Hydrometric Station Records, Field Stud. Res. Needs Science Report No. 2, Environment Canada, Inland Waters Directorate, National Water Research Institute, 1990.

Beltaos, S.: Onset of river ice breakup, Cold Reg. Sci. Technol., 25, 183–196, doi:10.1016/S0165-232X(96)00011-0, 1997.
Beltaos, S.: River ice breakup processes: recent advances and future directions, Can. J. Civil Eng., 34, 703–716, doi:10.1139/l06-021, 2007.
Beltaos, S.: Progress in the study and management of river ice jams, Cold Reg. Sci. Technol., 51, 2–19, 2008.
Beltaos, S.: Hydrodynamic characteristics and effects of river waves caused by ice jam releases, Cold Reg. Sci. Technol., 85, 42–55, doi:10.1016/j.coldregions.2012.08.003, 2013.
Beltaos, S. and Carter, T.: Field studies of ice breakup and jamming in lower Peace River, Canada, Cold Reg. Sci. Technol., 56, 102–114, doi:10.1016/j.coldregions.2008.11.002, 2009.
Beltaos, S. and Kääb, A.: Estimating river discharge during ice breakup from near-simultaneous satellite imagery, Cold Reg. Sci. Technol., 98, 35–46, 2014.
Beltaos, S. and Prowse, T.: River-ice hydrology in a shrinking cryosphere, Hydrol. Process., 23, 122–144, doi:10.1002/hyp.7165, 2009.
Beltaos, S., Rowsell, R., and Tang, P.: Remote data collection on ice breakup dynamics: Saint John River case study, Cold Reg. Sci. Technol., 67, 135–145, doi:10.1016/j.coldregions.2011.03.005, 2011.
Beltaos, S., Carter, T., and Rowsell, R.: Measurements and analysis of ice breakup and jamming characteristics in the Mackenzie Delta, Canada, Cold Reg. Sci. Technol., 82, 110–123, 2012.
Bigras, S. C.: Hydrological regime of lakes in the Mackenzie Delta, Northwest Territories, Canada, Arctic Alpine Res., 22, 163–174, doi:10.2307/1551301, 1990.
Bonsal, B. R. and Prowse, T. D.: Trends and variability in spring and autumn 0 °C-isotherm dates over Canada, Climate Change, 57, 341–358, doi:10.1023/A:1022810531237, 2003.
Brown, R. D. and Derksen, C.: Is Eurasian October snow cover extent increasing?, Environ. Res. Lett., 8, 024006, doi:10.1088/1748-9326/8/2/024006, 2013.
Brown, R. S., Stanislawski, S. S., and Mackay, W. C.: Effects of frazil ice on fish, in: Workshop on Environ, Aspects of River Ice, Saskatoon, Canada, National Hydrological Research Institute, Enir, Canada, 1994.
Brown, R. S., Power, G., Beltaos, S., and Beddow, T. A.: Effects of hanging ice dams on winter movements and swimming activity of fish, J. Fish Biol., 57, 1150–1159, doi:10.1111/j.1095-8649.2000.tb00477.x, 2000.

Chaouch, N., Temimi, M., Romanov, P., Cabrera, R., McKillop, G., and Khanbilvardi, R.: An automated algorithm for river ice monitoring over the Susquehanna River using the MODIS data, Hydrol. Process., 28, 62–73, doi:10.1002/hyp.9548, 2012.
Church, M.: Hydrology and Permafrost: With Reference to Northern North America, Permafrost Hydrology, 1974.
Dean, K. G., Stringer, W. J., Ahlnäs, K., Searcy, C., and Weingartner, T.: The influence of river discharge on the thawing of sea ice, Mackenzie River Delta: albedo and temperature analyses, Polar Res., 13, 83–94, doi:10.3402/polar.v13i1.6683, 1994.
de Rham, L. P., Prowse, T. D., Beltaos, S., and Lacroix, M. P.: Assessment of annual high-water events for the Mackenzie River basin, Canada, Hydrol. Process., 22, 3864–3880, doi:10.1002/hyp.7016, 2008a.
de Rham, L. P., Prowse, T. D., and Bonsal, B. R.: Temporal variations in river-ice break-up over the Mackenzie River Basin, Canada, J. Hydrol., 349, 441–454, doi:10.1016/j.jhydrol.2007.11.018, 2008b.
Gauthier, Y., El Battay, A., Bernier, M., and Ouarda, T.: An approach using contextual analysis to monitor river ice from RADARSAT data, in: Eastern Snow Conference, Sherbrooke, Québec, 151, 2003.
Goñi, M. A., Yunker, M. B., Macdonald, R. W., and Eglinton, T. I.: Distribution and sources of organic biomarkers in arctic sediments from the Mackenzie River and Beaufort Shelf, Mar. Chem., 71, 23–51, doi:10.1016/S0304-4203(00)00037-2, 2000.
Goulding, H. L., Prowse, T. D., and Beltaos, S.: Spatial and temporal patterns of break-up and ice-jam flooding in the Mackenzie Delta, NWT, Hydrol. Process., 23, 2654–2670, doi:10.1002/hyp.7251, 2009a.
Goulding, H. L., Prowse, T. D., and Bonsal, B.: Hydroclimatic controls on the occurrence of break-up and ice-jam flooding in the Mackenzie Delta, NWT, Canada, J. Hydrol., 379, 251–267, doi:10.1016/j.jhydrol.2009.10.006, 2009b.
Government of Canada, E. C.: Environment Canada – Water – About the Water Survey of Canada, available at: http://ec.gc.ca/rhc-wsc/default.asp?lang=En&n=EDA84EDA-1 (last access: 6 September 2014), 2007a.
Government of Canada, E. C.: Environment Canada – Water – Rivers, available at: http://www.ec.gc.ca/eau-water/default.asp?lang=En&n=45BBB7B8-1 (last access: 7 June 2014), 2007b.

TCD
9, 2783–2820, 2015

Monitoring ice break-up on the Mackenzie River using MODIS data

P. Muhammad et al.

Government of Canada, E. C.: Environment Canada – Water – Environment Canada Data Explorer, available at: http://www.ec.gc.ca/rhc-wsc/default.asp?lang=En&n=0A47D72F-1 (last access: 27 March 2013), 2010a.
Government of Canada, E. C.: Environment Canada – Water – Environment Canada Data Explorer, available at: http://www.ec.gc.ca/rhc-wsc/default.asp?lang=En&n=0A47D72F-1 (last access: 27 March 2013), 2010b.
Hall, D. D. K., Riggs, D. G. A., and Salomonson, D. V. V.: MODIS snow and sea ice products, in: Earth Science Satellite Remote Sensing, edited by: Qu, P. J. J., Gao, D. W., Kafatos, P. M., Murphy, D. R. E., and Salomonson, D. V. V., Springer, Berlin, Heidelberg, 154–181, 2006.
Harrop, C.: Covered bridge floats away, CBCca Play, available at: http://www.cbc.ca/player/News/Canada/NB/ID/2449841279/#, last access: 25 May 2014.
Hicks, F.: An overview of river ice problems: CRIPE07 guest editorial, Cold Reg. Sci. Technol., 55, 175–185, 2009.
Hicks, F., Cui, W., and Ashton, G.: River ice breakup, in: Heat Transfer and Ice Cover Decay, chapter 4, Water Resources Pubns, Highlands Ranch, CO, 2008.
Hicks, F. E., Cui, W., Andres, D. D., and Territories, N.: Forecasting breakup on the Mackenzie River at the Ft. Providence Ferry Crossing, University of Alberta, Kamloops, BC, 1995.
Jasek, M., Marko, J., Fissel, D., Clarke, M., Buermans, J., and Paslawski, K.: Instrument for detecting freeze-up, mid-winter and break-up ice processes in rivers, in: Proc. 13th Workshop on River Ice, CGU-HS CRIPE, Hanover, 151–183, 2005.
Kääb, A. and Prowse, T.: Cold-regions river flow observed from space, Geophys. Res. Lett., 38, L08403, doi:10.1029/2011GL047022, 2011.
Kääb, A., Lamare, M., and Abrams, M.: River ice flux and water velocities along a 600 km-long reach of Lena River, Siberia, from satellite stereo, Hydrol. Earth Syst. Sci., 17, 4671–4683, doi:10.5194/hess-17-4671-2013, 2013.
Kowalczyk Hutchison, T. and Hicks, F. E.: Observations of ice jam release waves on the Athabasca River near Fort Mcmurray, Alberta, Can. J. Civil Eng., 34, 473–484, 2007.
Lacroix, M., Prowse, T., Bonsal, B., Duguay, C., and Ménard, P.: River ice trends in Canada, in: Proc. 13th Workshop Hydraul. Ice Cover, Rivers CGU HS Comm. River Ice Process. Environ. CRIPE, Hanover, NH, 15–16, 2005.
Lenormand, F., Duguay, C. R., and Gauthier, R.: Development of a historical ice database for the study of climate change in Canada, Hydrol. Process., 16, 3707–3722, 2002.
Lock, G. S. H.: The Growth and Decay of Ice, Cambridge University Press, 1990.

MacKay, D. K.: Mackenzie River and Delta ice survey, 1965, Geogr. Bull., 8, 270–278, 1966.
MacKay, D. K. and Mackay, J. R.: Locations of Spring Ice Jamming on the Mackenzie River, N. W. T. Environ.-Soc. Com. North. Pipelines Task Force North. Oil Dev. Rep. No. 73-3 Technical Report 8, North Pipelines Task Force North, Ottowa, 1973.
Magnuson, J. J., Robertson, D. M., Benson, B. J., Wynne, R. H., Livingstone, D. M., Arai, T., Assel, R. A., Barry, R. G., Card, V., Kuusisto, E., Granin, N. G., Prowse, T. D., Stewart, K. M., and Vuglinski, V. S.: Historical trends in lake and river Ice cover in the Northern Hemisphere, Science, 289, 1743–1746, doi:10.1126/science.289.5485.1743, 2000.
Marsh, P. and Hey, M.: Analysis of spring high water events in the Mackenzie Delta and implications for lake and terrestrial flooding, Geogr. Ann. Ser. Phys. Geogr., 76, 221–234, 1994.
Marsh, P. and Prowse, T. D.: Water temperature and heat flux at the base of river ice covers, Cold Reg. Sci. Technol., 14, 33–50, doi:10.1016/0165-232X(87)90042-5, 1987.
Mermoz, S., Allain-Bailhache, S., Bernier, M., Pottier, E., Van Der Sanden, J. J., and Chokmani, K.: Retrieval of river Ice thickness from C-Band PolSAR data, IEEE T. Geosci. Remote, 52, 3052–3062, doi:10.1109/TGRS.2013.2269014, 2014.
Michel, B.: Limit equilibrium of ice jams, Cold Reg. Sci. Technol., 20, 107–117, 1992.
Nghiem, S. V., Hall, D. K., Rigor, I. G., Li, P., and Neumann, G.: Effects of Mackenzie River discharge and bathymetry on sea ice in the Beaufort Sea, Geophys. Res. Lett., 41, 873–879, 2014.
Pavelsky, T. M. and Smith, L. C.: Spatial and temporal patterns in Arctic river ice breakup observed with MODIS and AVHRR time series, Remote Sens. Environ., 93, 328–338, doi:10.1016/j.rse.2004.07.018, 2004.
Province of Manitoba, E. C.: Manitoba – Flood Information, available at: http://www.gov.mb.ca/flooding/history/index.html (last access: 11 June 2014), 2011.
Prowse, T. D.: Environmental significance of ice to streamflow in cold regions, Freshwater Biol., 32, 241–259, doi:10.1111/j.1365-2427.1994.tb01124.x, 1994.
Prowse, T. D.: River-ice ecology. I: Hydrologic, geomorphic, and water-quality aspects, J. Cold Reg. Eng., 15, 1–16, doi:10.1061/(ASCE)0887-381X(2001)15:1(1), 2001.
Prowse, T. D. and Beltaos, S.: Climatic control of river-ice hydrology: a review, Hydrol. Process., 16, 805–822, doi:10.1002/hyp.369, 2002.
Prowse, T. D. and Carter, T.: Significance of ice-induced storage to spring runoff: a case study of the Mackenzie River, Hydrol. Process., 16, 779–788, doi:10.1002/hyp.371, 2002.

TCD
9, 2783–2820, 2015

Prowse, T. D. and Marsh, P.: Thermal budget of river ice covers during breakup, Can. J. Civil Eng., 16, 62–71, doi:10.1139/l89-008, 1989.
Riggs, G. A., Barton, J. S., Casey, K. A., Hall, D. K., and Salomonson, V. V.: MODIS Snow Products Users' Guide, NASA GSFC, 2000.
Scrimgeour, G. J., Prowse, T. D., Culp, J. M., and Chambers, P. A.: Ecological effects of river ice break-up: a review and perspective, Freshwater Biol., 32, 261–275, doi:10.1111/j.1365-2427.1994.tb01125.x, 1994.
Shen, H. T. and Liu, L.: Shokotsu River ice jam formation, Cold Reg. Sci. Technol., 37, 35–49, doi:10.1016/S0165-232X(03)00034-X, 2003.
Shiklomanov, A. I. and Lammers, R. B.: River ice responses to a warming Arctic – recent evidence from Russian rivers, Environ. Res. Lett., 9, 035008, doi:10.1088/1748-9326/9/3/035008, 2014.
Stewart, R. E., Crawford, R. W., Leighton, H. G., Marsh, P., Strong, G. S., Moore, G. W. K., Ritchie, H., Rouse, W. R., Soulis, E. D., and Kochtubajda, B.: The Mackenzie GEWEX Study: the water and energy cycles of a major North American river basin, B. Am. Meteorol. Soc., 79, 2665–2683, 1998.
Terroux, A. C. D., Sherstone, D. A., Kent, T. D., Anderson, J. C., Bigras, S. C., and Kriwoken, L. A.: Ice regime of the lower Mackenzie River and Mackenzie Delta, Environ. Can. Natl. Hydrol. Res. Inst., Hull, Quebec, 1981.
Unterschultz, K. D., van der Sanden, J., and Hicks, F. E.: Potential of RADARSAT-1 for the monitoring of river ice: results of a case study on the Athabasca River at Fort McMurray, Canada, Cold Reg. Sci. Technol., 55, 238–248, doi:10.1016/j.coldregions.2008.02.003, 2009.
White, K. D., Hicks, F., Beltaos, S., and Loss, G.: Ice jam response and mitigation: the need for cooperative succession planning and knowledge transfer, in: Proc. 14th Workshop on River Ice, Quebec City, Quebec, Canada, 20–22, 2007.
Woo, M.-K.: Cold region atmospheric and hydrologic studies the Mackenzie gewex experience, Springer, Berlin, New York, 2008.
Woo, M.-K. and Thorne, R.: Streamflow in the Mackenzie Basin, Canada, Arctic, 56, 328–340, 2003.

TCD
9, 2783–2820, 2015

Title Page
Abstract | Introduction
Conclusions | References
Tables | Figures
◀| |▶
◀ ▶
Back | Close
Full Screen / Esc
Printer-friendly Version
Interactive Discussion

TCD
9, 2783–2820, 2015

Monitoring ice break-up on the Mackenzie River using MODIS data

P. Muhammad et al.

Table 1. Description of Water Survey of Canada hydrometric stations on the Mackenzie River.

Station Name	Coordinates	Distances downstream from the western end of Great Slave Lake
Mackenzie River at Fort Providence	61.27° N, 117.54° W	75.8 km
Mackenzie River at Strong Point	61.81° N, 120.79° W	301 km
Mackenzie River at Fort Simpson	61.86° N, 121.35° W	330 km
Mackenzie River at Norman Wells	65.27° N, 126.84° W	890 km
Mackenzie River at Arctic Red River	67.45° N, 133. 75° W	1435 km

Table 2. Scientific data set (SDS) and digital number (DN) values from MODIS L1B and L3 products used for the Mackenzie River.

Image Cover	MOD/MYD L3 (SDS) (500 m)	MOD/MYD L1B (DN) (250 m)
Cloud Cover	50	150 <
Snow	200	111–150
Ice (Snow Covered)	100	40–110
Open Water	37	30
Land	25	< 28

TCD
9, 2783–2820, 2015

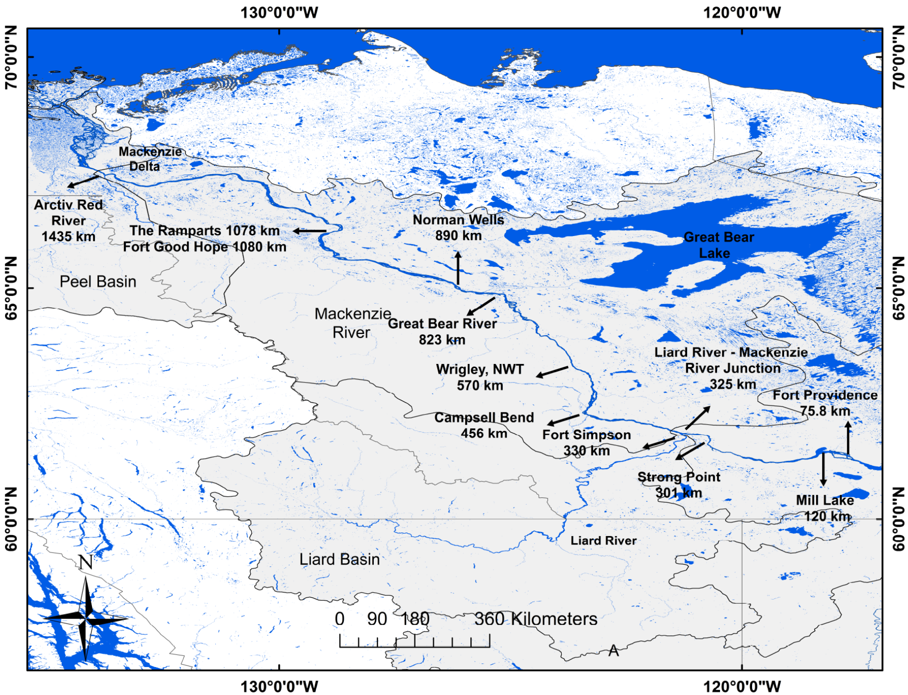

Figure 1. Northern reaches of the Mackenzie River Basin (MRB), its sub-basins and major rivers and lakes. The MRB extends from 54 to 68° N flowing from the southeast to northwest. The names of sub-basins and tributaries feeding into the Mackenzie River as well (marked by arrows) distances from western end of Great Slave Lake are also shown.

TCD
9, 2783–2820, 2015

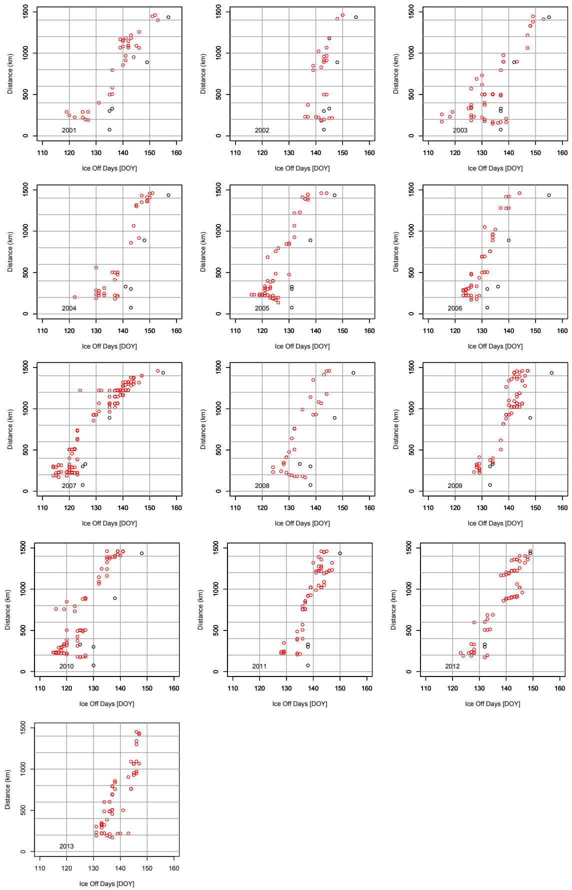

Figure 2. Estimated ice-off dates as illustrated by the red circles between 2001–2013 on the MR. Terra observations were made throughout the study period, while Aqua observations were available from 2003-onward. Black circles are indicative of WSC ice observation dates.

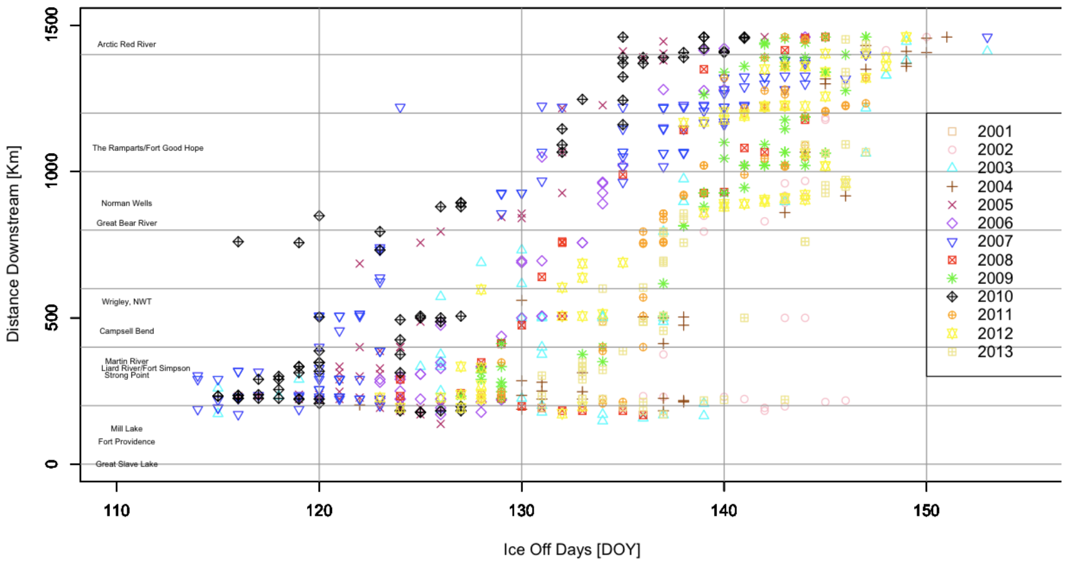

Figure 3. Compilation of all ice-off dates from 2001 to 2013 DOY [Day of Year] on the MR. First ice break-up dates generally began near 325 km. Ice break-up processes are more protracted just south of 325 km as seen with the higher density of measurements. Near 1078 km, a second channel constriction is present giving rise to two distinct ice-run patterns.

TCD
9, 2783–2820, 2015

Title Page
Abstract | Introduction
Conclusions | References
Tables | Figures
◂◂ | ▸▸
◂ | ▸
Back | Close
Full Screen / Esc
Printer-friendly Version
Interactive Discussion

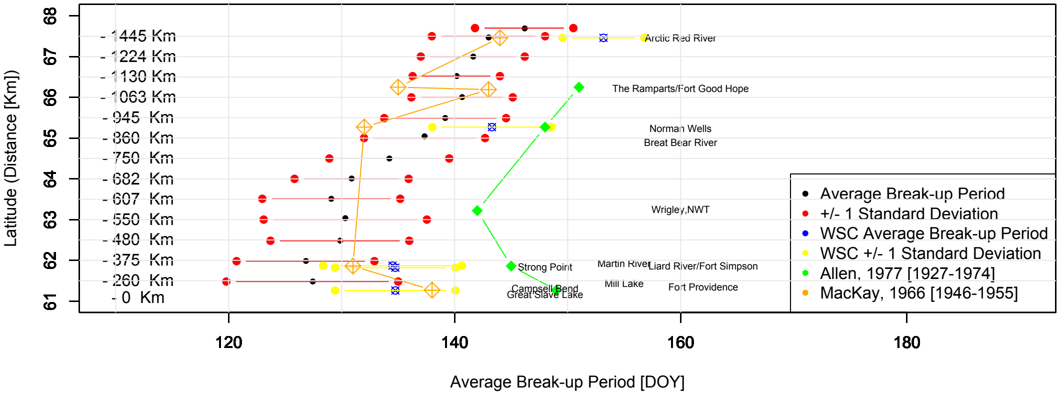

Figure 4. Average ice break-up dates estimated from MODIS (2001–2013) are given by the black dots, with ± one SD showed with the red dots. The blue dots illustrate the WSC average ice break-up dates and the yellow dots ± one SD. The green and orange dots represent average ice break-up dates from Allen (1977) from the time period of 1927 to 1974 and MacKay (1966) from the time period of 1946 to 1955, respectively.

TCD
9, 2783–2820, 2015

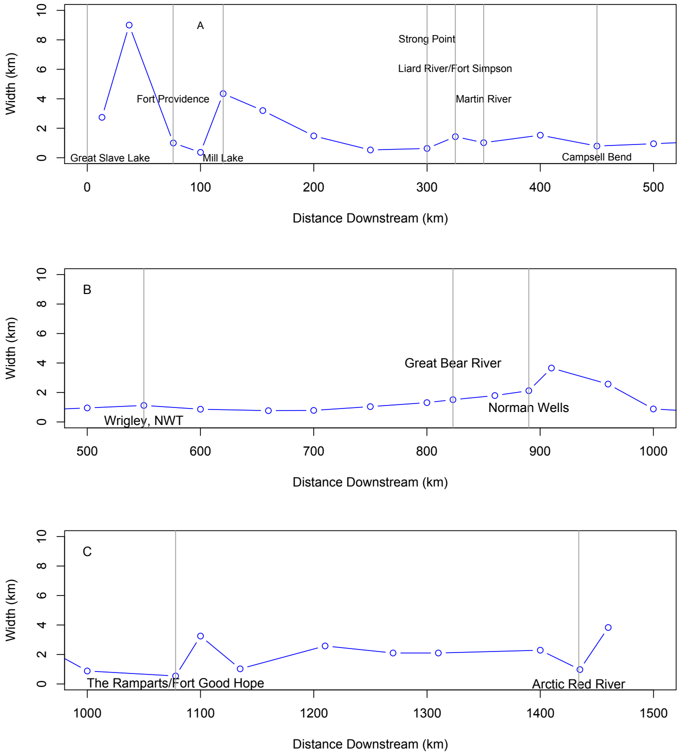

Figure 5. Change in channel width along the Mackenzie River as observed in **(a)** (ca. 0–500 km), **(b)** (ca. 500–1000 km) and **(c)** (ca. 1000–1500 km).

TCD
9, 2783–2820, 2015

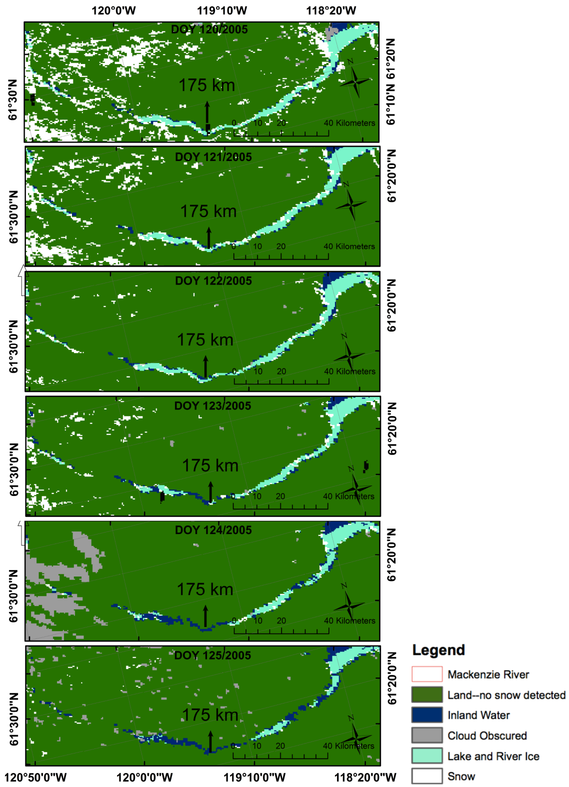

Figure 6. This example illustrates ice break-up at the headwaters of the Mackenzie River system in 2005 from DOY 120–125.

TCD
9, 2783–2820, 2015

Monitoring ice break-up on the Mackenzie River using MODIS data

P. Muhammad et al.

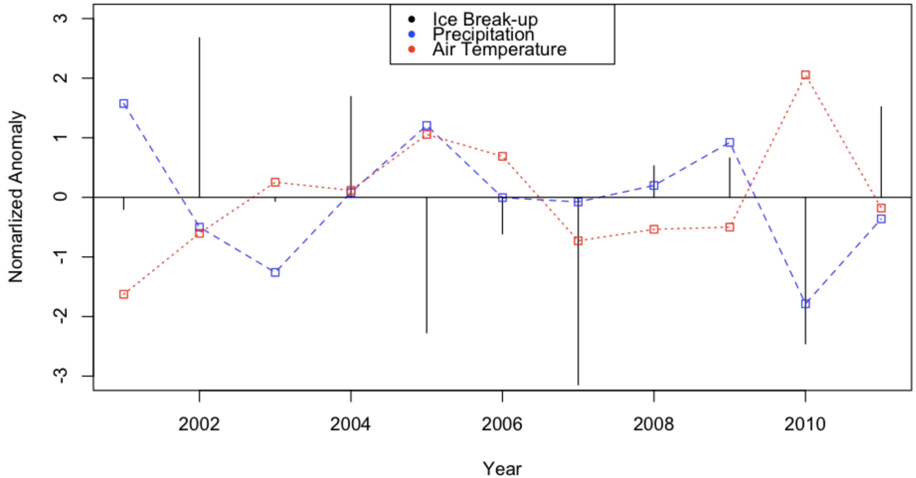

Figure 7. Normalized anomalies of ice break-up dates estimated with MODIS (black lines), together with precipitation (blue dots) and air temperature (red squares) determined from ERA monthly means (January to March) for the period 2001–2011. The average ice break-up date is DOY 128 at 62.5° N, precipitation is 314.1 mm and air temperature is −14.4 °C.

TCD
9, 2783–2820, 2015

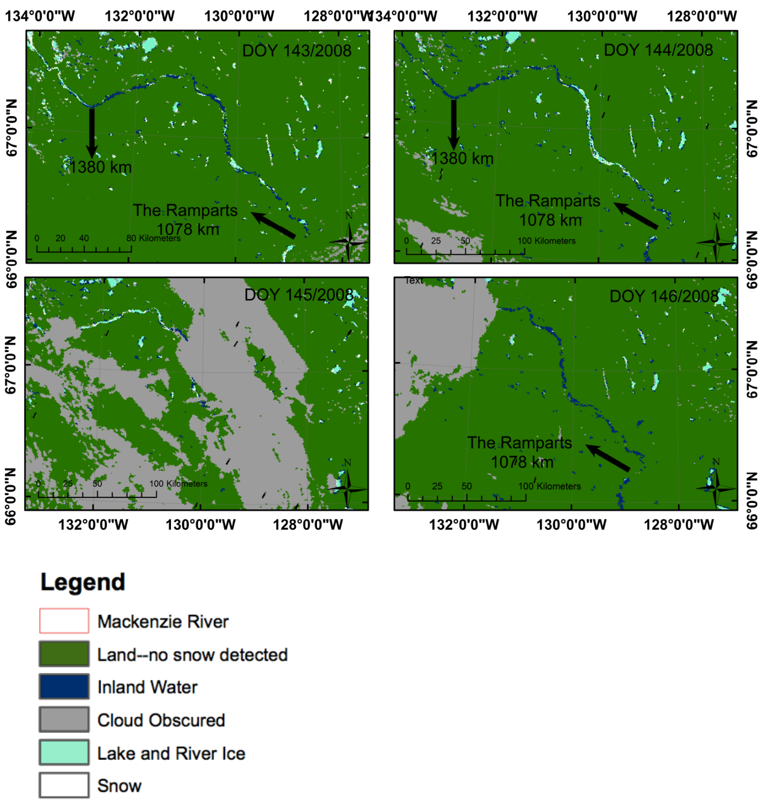

Figure 8. Ice flushing event recorded in 2008 between DOY 143–146.

TCD
9, 2783–2820, 2015

Monitoring ice break-up on the Mackenzie River using MODIS data

P. Muhammad et al.

Title Page
Abstract | Introduction
Conclusions | References
Tables | Figures
◀| |▶
◀ ▶
Back | Close
Full Screen / Esc
Printer-friendly Version
Interactive Discussion

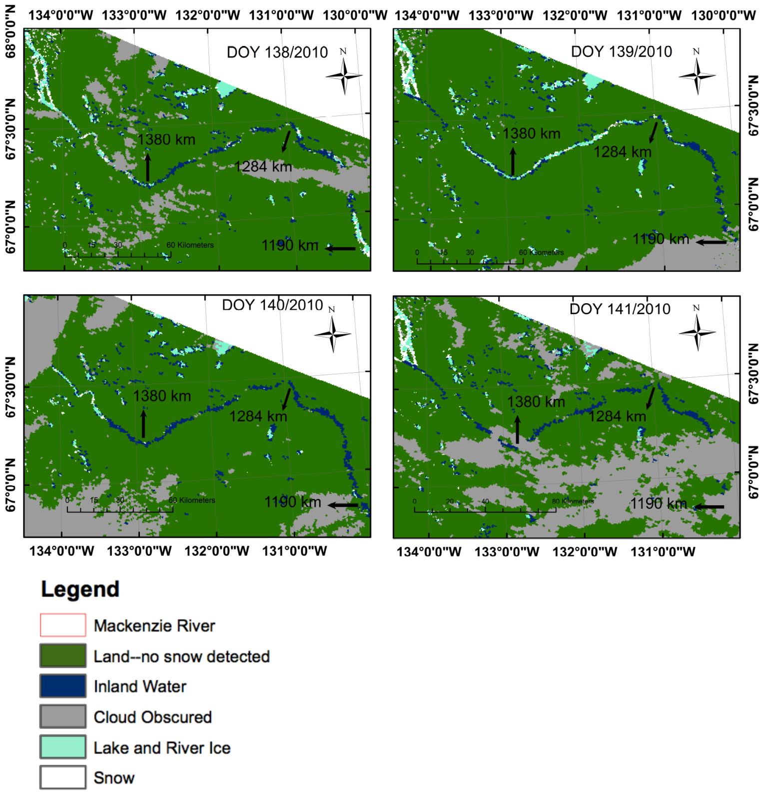

Figure 9. Ice flushing event recorded in 2010 between DOY 138–141. Here, on DOY 141, the ice movement is last recorded after existing into the Mackenzie Delta.

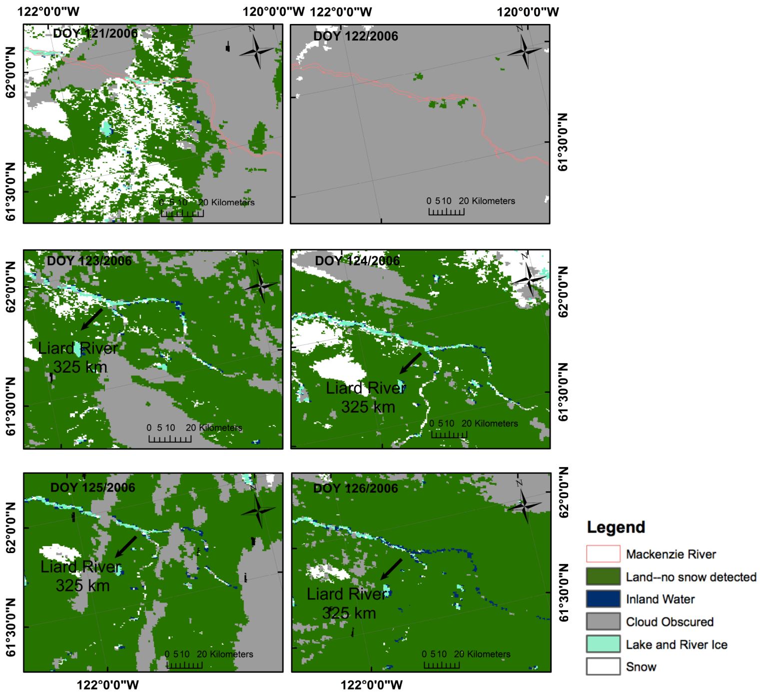

Figure 10. As example of thermodynamic break-up, where ice within the river requires an extra 2–3 days to be cleared after snow has melted over the immediate drainage basin. This example was observed in 2006 between DOY 121–126.

TCD
9, 2783–2820, 2015

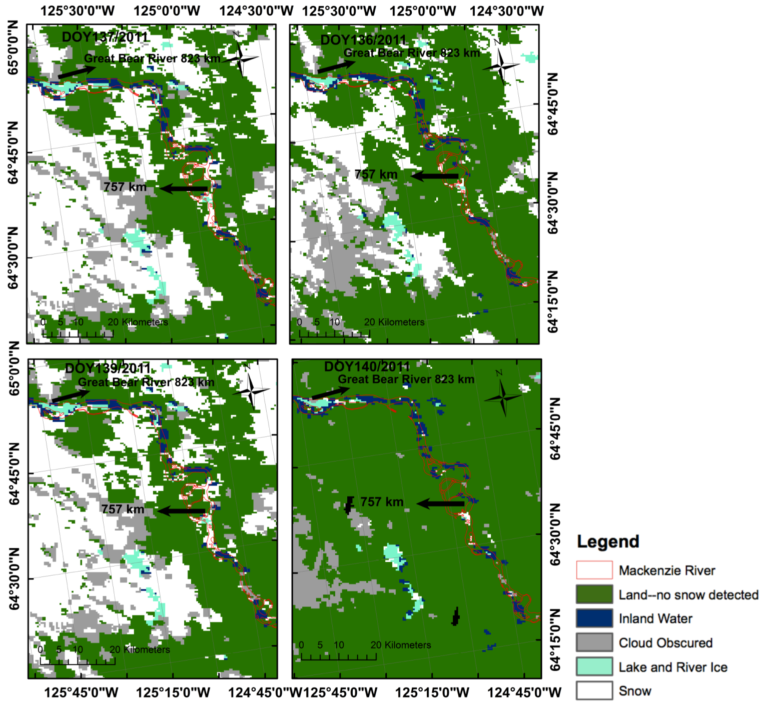

Figure 11. Snowmelt and ice run over the MRB in 2011 between the DOY 137–140. There is a 2 day lag between the complete clearance of snow on land and the clearance of ice on the Mackenzie River.

TCD
9, 2783–2820, 2015

Monitoring ice break-up on the Mackenzie River using MODIS data

P. Muhammad et al.

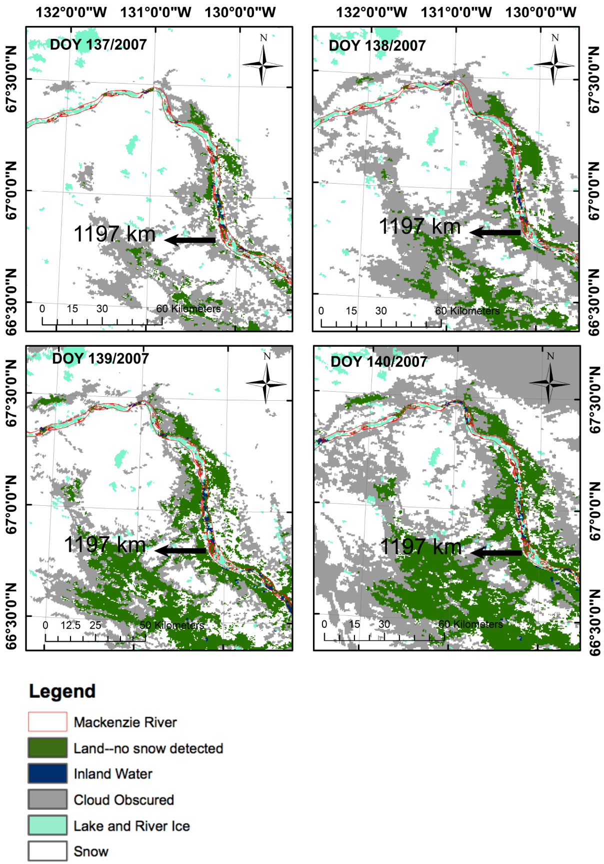

Figure 12. Observation of dynamic break-up over a section of the MRB, showing concurrent ice break-up and snowmelt over 6 days. This was observed in 2007 between DOY 137–142.